engineering proceedings

MDPI

Proceeding Paper

Optical Centroid Efficiency in Infrared Sensors †

Marija Strojnik [1,*] and Yaujen Wang [2,‡]

[1] Optical Research, Apdo. Postal 948, Leon 37000, Mexico
[2] Independent Researcher, Arcadia, CA 91006, USA; lightw123@gmail.com
* Correspondence: mstrojnik@gmail.com; Tel.: +1-(480)-479-7817
† Presented at the 17th International Workshop on Advanced Infrared Technology and Applications, Venice, Italy, 10–13 September 2023.
‡ Portion of this work was performed when the author was affiliated with Northrop Grumman, Aerospace Systems, Azusa, CA 91702, USA.

Abstract: The noise-equivalent power is used to predict performance of infrared (IR) sensors. In a general IR or remote sensing system, the axes of the incoming chief ray of each pixel in the optical system and the center of that detector pixel are slightly misaligned, due to optical tolerances, jitter, and other environmental conditions, leading to error in the sensor performance prediction and estimates. A new figure-of-merit, the optical centroid efficiency (*OCE*), considers the energy on the rectangular detector pixel, averaged over all positions on the pixel. We calculate the *OCE* as a function of energy on detector (EOD) for a popular IR imaging system, a three-mirror reflector.

Keywords: optical centroid efficiency; *OCE*; ensquared energy (energy on detector; *EOD*); sensors; infrared; numerical simulations; remote-sensing instruments

Citation: Strojnik, M.; Wang, Y. Optical Centroid Efficiency in Infrared Sensors. *Eng. Proc.* **2023**, *51*, 40. https://doi.org/10.3390/engproc2023051040

Academic Editors: Gianluca Cadelano, Giovanni Ferrarini and Davide Moroni

Published: 7 December 2023

1. Energy Interception by Discrete, Rectangular Pixels

When an image was detected with the photographic emulsion, the instrument resolution was defined by the optical system. The energy enclosed within a circle, the enclosed energy, was deemed sufficient to define such derived concepts as noise-equivalent power (NEP), used as a basis of most other derived figures of merit [1]. They were derived for the IR spectrum, and applied in the visible spectrum when radiometric quantities were used in the analysis. The concept of the energy captured by a rectangular detector (*EOD*) has become important when rectangular pixel arrays were introduced [2–4].

The sensor performance evaluations up to now have not included the detector pixel dimensions because the detector pixel size was usually chosen after the geometry of the optical system aperture. If an object shape was to be identified, then several pixels would be selected across the diameter of the Airy disc. If large Earth-surface areas were imaged eliminate paragraph indentin remote sensing, the consideration was on the amount of collected energy with the expectation that extrapolation between pixels would lead to subpixel image interpolation.

The EOD_d is a multiplicative correction factor that was invoked in the instrument design to account for the asymmetrical spread of an image of a point source over several detector pixels, in the case that the pixel is decentered by $(\Delta d_x,\Delta d_y)$ with respect to the axis of the optical system. The optical centroiding efficiency $OCE(d_x,d_y)$ may be considered the normalized $EOD_d(d_x,d_y)$, averaged over a detector area.

The minimum normalized energy on the detector must be greater than 0.25 when the axis of the optical system is misaligned to the pixel's furthest diagonal point by $(\Delta d_x,\Delta d_y) = (d,d)$. In this limiting case, the image of a diffraction-limited spot spreads to four pixels. This represents an ineffective use of detector technology. When the misalignment happens along a single dimension, for example, along $\Delta d_x = \Delta d_y = d$, the image of a diffraction-limited spot spreads to two pixels along the direction of misalignment, similarly

resulting in the reduction in energy on the detector to a maximum of 0.5. This represents a similarly ineffective use of the detector resources. Both displacements result in the decrease in the signal-to-noise ratio and in the decrease in the instrument resolution. The latter case also introduces image distortion, characteristic of the astigmatism. When considering the possibility of such a displacement that might result in a potential energy capture of 0.5, it is advantageous to quadruple the detector size. In an imaging instrument, the energy on the detector must not fall below 0.5 to assure similarity of the image to the object.

Up until now, the instrument figure-of-merit for the combined optical system and detector pixel in IR has not been formulated. We attempt to do so in this summary.

2. Effects of Pixel Size and Central Obscuration on the *OCE*

We previously analyzed the *OCE* for two aperture types: an ideal circular aperture of diameter *D* and an ideal circular aperture with a rectangular central obscuration. A rectangular obscuration is at first sight absent in the telescope and remote sensing instruments. The James Webb Space Telescope, though, features an aperture with edges formed by sides of hexagons. For its individual hexagonal segments prior to phasing, the central hole is formed by six straight edges at 0-, $\pi/3$-, $2\pi/3$-, $\pi-$, $4\pi/3$-, or $5\pi/3$-angles with respect to the orientation of each surrounding segment ring.

Only for large pixel sizes, of more than 4 (λF/#), the shape of the curve *OCE*-vs.-pixel-size starts to increase in a monotonical fashion for an optical instrument with a generalized rectangular obscuration. For smaller values of pixel size, between 2.2 and 4 (λF/#), the *OCE* vs. pixel size decreases with the increasing pixel size. We consider such behavior anomalous, as the *OCE* is just an average of the *EOD* over the pixel surface. For still smaller pixel values, the *OCE* again increases with the pixel size, as expected.

In the absence of the central obscuration, the *OCE* increases with the pixel size, same as the *EOD* increases with pixel size. The presence of the central obscuration introduces an anomaly in the *OCE* vs. pixel size. Thus, we may conclude that the effect of the central obscuration is to decrease the region of the pixel sizes where the *OCT* increases with the pixel size to those larger than about 4 (λF/#).

We next examine the *OCE* vs. *EOD* for a single imaging optical component with a mixture of aberrations, dominated by the spherical aberration.

3. Imaging Optical Component, Having a Combination of Aberrations

We next assess the effects of aberrations on the relationship between the *OCE* and *EOD* for a mix of aberrations as follows: Spherical to coma to astigmatism = (1:0.25:0.25). In the presence of a unit wave of spherical aberration in an optical sensor, the accompanying coma and astigmatism is 0.25 waves each. The relationships between the *OCE* and the *EOD* for this component are presented in Figure 1 for (a) 2d = (3λF/#) and (b) 2d = (7λF/#).

Next, we extend the analysis of the *OCE* vs. *EOD* from a single imaging component to a reflective imaging system, often employed in IR remote sensing instruments.

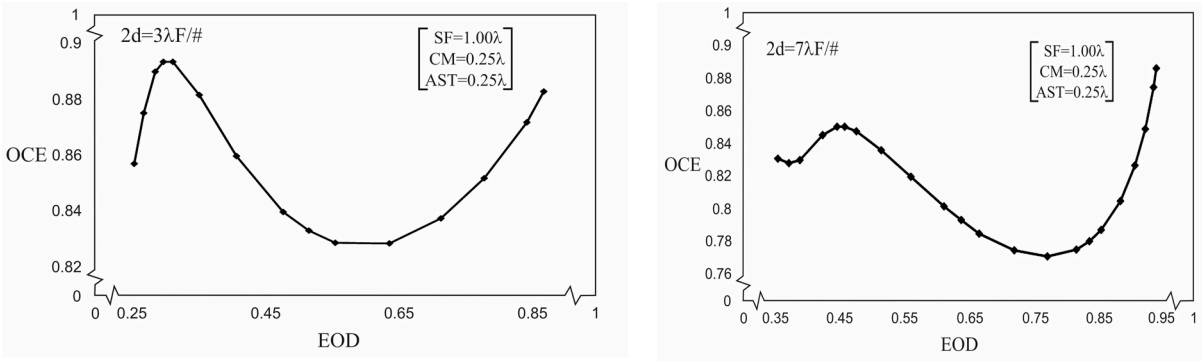

(**a**) 2d = (3λF/#) (**b**) 2d = (7λF/#)

Figure 1. The *OCE* as a function of *EOD* for an imaging component, with the proportion of aberrations, Spherical to coma to astigmatism = (1:0.25:0.25) for detector pixel sizes (**a**) 2d = (3λF/#) and (**b**) 2d = (7λF/#). In the absence of aberration, the pixel in Figure (**a**) comfortably encloses 1 Airy disc, while the pixel in Figure (**b**) encloses 3. In this diagram, the amount of aberrations, going from the maximum (1.0, 0.25, 0.25) λ to zero (0), decreases from left to right implicitly along the *EOD*-axis.

4. Reflective Three-Mirror (RTM) System

In IR instruments, the reflective optical systems are preferred because they can be lightweighted, they feature minimal transmission loss, and they undergo simplified coating processes. Additionally, they avoid the chromatic aberration that is introduced in wide spectral intervals and minimize the Fresnel losses at the component boundaries. The *OCE* anomaly further provides diffraction-related information about desirability of the all-reflective instrument concepts in IR.

A reflective three-mirror (*RTM*) optical/IR system is often used in remote sensing instruments [5,6] as well as in military surveillance systems. As a practical instrument, we analyze a real design of the optical system, presented in Figure 2 [6]. This three-mirror all-reflective F/2 optical system features, for example, a moderate full field of view of 4.5° multiplied by 4.5°. After reflection at the third mirror, the incoming beam is reflected by the front surface of a dichroic beam splitter (the transmission channel for different wavelengths is not presented). Finally, the light beam passes through a filter and then reaches the FPA.

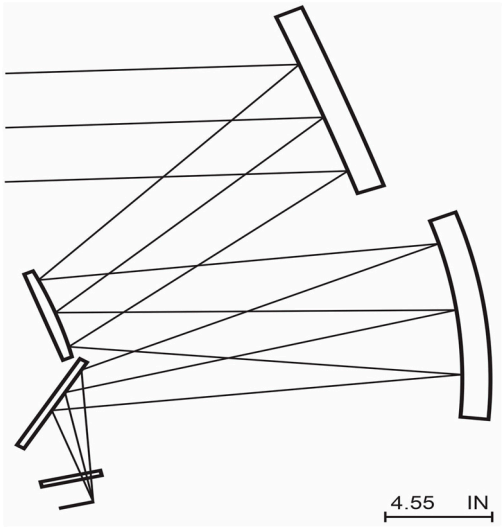

Figure 2. Optical layout of the RTM.

The relationships between the *OCE* and the *EOD* for the RMT of Figure 2 are presented in Figure 3 for the detector sizes, (a) 2d = (3λF/#) and (b) 2d = (7λF/#). For each value of the *EOD*, we always maintain an aberration ratio of Spherical to coma to astigmatism in

proportion (1:0.25:0.25) as *EOD* increases. The maximum aberration mix is (1.0, 0.25, 0.25) λ for low values of *EOD*.

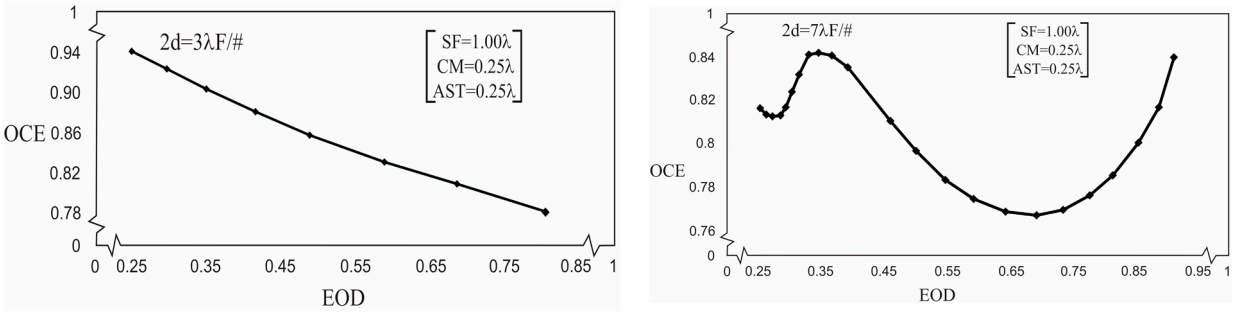

(**a**) 2d = (3λF/#) (**b**) 2d = (7λF/#)

Figure 3. The *OCE* as a function of the *EOD* for the RTM of Figure 2, with the proportion of aberrations, Spherical to coma to astigmatism = (1:0.25:0.25) for detector pixel sizes (**a**) 2d = (3λF/#) and (**b**) 2d = (7λF/#). In the absence of aberration, the pixel in (**a**) comfortably encloses 1 Airy disc, while the pixel in (**b**) encloses 3. In this diagram, the amount of aberrations, going from the maximum (1.0, 0.25, 0.25) λ to zero (0), decreases from left to right implicitly along the *EOD*-axis.

5. Conclusions

We introduced the optical centroid efficiency as a figure-of-merit to account for misalignment, produced by jitter and other environmental conditions. The pupil geometry-driven diffraction patterns incident on the pixel result in the rise in additional features in the shape of the *OCE*-vs.-*EOD* curves. The *EOD* analysis indicates that even for static cases of misalignment, the instruments with *EOD* smaller than 0.5 result in the image washout.

The *OCE* as a figure-of-merit is appropriate for the instruments whose detector pixel is larger than or equal to the aberrated image diameter of a point object in infinity.

We presented a special case of the *OCE*-vs.-*EOD* calculations for an all-reflective three-mirror system, TRM, one of the highly popular remote sensing/surveillance optical/IR configurations, with a mixture of three primary aberrations. The anomalous negative slope of the *OCE*-vs.-*EOD* curve for the TRM for the small pixel size, 2d = (3λF/#), indicates that this pixel size is too small for the magnitude of aberrations in this system. This result indicates an important area where the *OCE* may be used to specify the instrument performance parameters.

For the electro-optical IR systems with anticipated jitter, larger pixel sizes (double the dimeter of Airy disc) result in the same instrument imaging resolution. Equivalently, an about 20% higher S/N ratio must be included as the design requirement to resolve the point source in infinity. For the instruments with a mix of aberrations, the anomalous behavior of the *OCE*, being inversely proportional to the *EOD*, is exhibited for the small pixel size. This indicates that a pixel, smaller than the aberrated image of the point object at infinity, is not an optimized component for the inclusion into an instrument with relatively large amounts of aberrations. A pixel of a larger size would result in a better instrument optimization, cost-effective design, and some compromise in performance, as measured by the effective image resolution and signal detection.

In conclusion, this work clearly indicates the relationship between the *OCE* and the *EOD* for electro-optical IR systems as follows: (1) The conventional wisdom of either a constant value of *OCE* or *OCE* increasing when the *EOD* increases is unrealistic. (2) Our assumptions of the aberration ratio used in the computations are for reference only. (3) Finally, in a sensor of a given pixel size and shape and with reasonable aberration information, the above procedure can indeed provide an accurate relationship between the *OCE* and the *EOD*. Therefore, such early evaluations are expected to lead to better understanding, performance prediction, and potential cost tradeoffs for the instrument during the preliminary design stage.

Author Contributions: Conceptualization, Y.W.; modeling, Y.W.; software, Y.W.; validation, M.S.; formal analysis, M.S.; investigation, M.S.; writing—original writing, review, and editing, M.S.; visualization, M.S. All authors have read and agreed to the published version of the manuscript.

Funding: This research received no external funding.

Institutional Review Board Statement: Not applicable.

Informed Consent Statement: Not applicable.

Data Availability Statement: Data are included in the paper.

Conflicts of Interest: Authors declare no conflict of interest.

References

1. Mackowiak, V.; Peupelmann, J.; Ma, Y.; Gorges, A. NEP—Noise Equivalent Power, ThorLabs. Available online: https://www.thorlabs.com/images/ (accessed on 18 June 2023).
2. Beyer, L.M.; Cobb, S.H.; Clune, L.C. Ensquared power for obscured circular pupils with off-center imaging. *Appl. Opt.* **1991**, *30*, 3569. [CrossRef] [PubMed]
3. Holst, G. *Electro-Optical Imaging System Performance*, 3rd ed.; SPIE: Washington, DC, USA, 2002; p. 204.
4. Lloyd, J.M. *Thermal Imaging Systems*; Plenum Press: New York, NY, USA, 1975; pp. 11–166.
5. Strojnik, M.; Bravo-Medina, M.B.; Beltran-Gonzalez, A.; Wang, Y. Off-axis three-mirror optical system designs: From Cooke's triplet to remote sensing and surveying Instruments. *Appl. Sci.* **2023**, *13*, 8866. [CrossRef]
6. Wang, Y. Dichroic Beam Splitter and Related Apparatus and Methods. U.S. Patent 7,616,378, 10 November 2009.